Materials Science & Engineering A 658 (2016) 415–421

Contents lists available at ScienceDirect

Materials Science & Engineering A

journal homepage: www.elsevier.com/locate/msea

Indentation creep behavior of cold sprayed aluminum amorphous/nano-crystalline coatings

P. Suresh Babu [a,b], R. Jha [b], M. Guzman [b], G. Sundararajan [a], Arvind Agarwal [b,*]

[a] International Advanced Research Centre for Powder Metallurgy and New Materials (ARCI), Balapur, Hyderabad 500005, Andhra Pradesh, India
[b] Nanomechanics and Nanotribology Laboratory, Department of Mechanical and Materials Engineering, Florida International University, Miami, FL 33174, USA

ARTICLE INFO

Article history:
Received 13 August 2015
Received in revised form
8 February 2016
Accepted 9 February 2016
Available online 10 February 2016

Keywords:
Cold spray
Aluminum amorphous alloy
Nano-indentation creep
Stress exponent
Activation volume

ABSTRACT

In this study, we report room temperature creep properties of cold sprayed aluminum amorphous/nanocrystalline coating using nanoindentation technique. Creep experiments were also performed on heat treated coatings to study the structural stability and its influence on the creep behavior. The peak load and holding time were varied from 1000 to 4000 μN and 0 to 240 s respectively. Stress exponent value (n) vary from 5.6 to 2.3 in as-sprayed (AS) coatings and 7.2–4.8 in heat treated (HT) coatings at peak load of 1000–4000 μN at 240 s hold time. Higher stress exponent value indicates heat treated coatings have more resistance to creep deformation than as-sprayed coatings. Relaxed, partially crystallized structure with less porosity, and stronger inter-splat boundaries restrict the deformation in heat treated coatings as compared to greater free volume generation in amorphous as-sprayed coatings. The computed activation volume of heat treated coatings is twice of as-sprayed coatings indicating greater number of atom participation in shear band formation in heat treated coatings. The proposed mechanism was found to be consistent with the stress exponent values.

1. Introduction

Bulk metallic glasses (BMG) exhibit unique mechanical properties and high potential for applications such as advanced structural and functional materials [1]. Due to their high-strength, high elastic limit and excellent corrosion resistance, BMGs have attracted increasing interest in the research community [2,3]. In particular, Aluminum based BMGs have excellent properties as compared to their crystalline counterparts [4–6]. Al-BMGs have exhibited high strength (above 1000 MPa, 3–4 times higher than crystalline counter parts), low density (3.2–3.7 g/cm^3) and better corrosion and wear properties [7–10]. Additionally, multi-components in Al amorphous alloys enhance the glass forming ability and super cooled liquid region to obtain the thick glassy structure components with relatively low cooling rates [10]. Further, the presence of nano α-Al (FCC) phase in the glass matrix of Al-BMGs increases strength up to 1500 MPa [11,12].

The use of nanoindentation for the creep characterization of bulk metallic glasses (BMGs) has increased in the past few years. In such tests, the sample may be prepared easily and only a small piece of the specimen is sufficient for accurate measurements, thus rendering this particular technique attractive and advantageous [13]. Nanoindentation creep studies have been carried out on most common La, Ce, Ti, Fe, Zr, Cu, Mg based BMGs [13–18]. The creep displacement has been observed in both low (La, Ce) and high (Fe, Zr) glass transition (T_g) BMGs in room temperature creep tests [13,16]. An increase in creep displacement with an increase in the peak hold load and loading rate at same peak load were reported [14,15,17–19]. In order to understand the creep behavior of BMGs, creep displacement as a function of hold period has been analyzed and stress exponent factor (n) has been computed. An increase in stress exponent factor (n) with an increase in the load and a decrease in 'n' with increase in strain rate was observed in Fe-BMGs [14,15,17]. However, an opposite trend was noticed in Cu-Zr BMGs [20]. Wang et al. reported strain rate sensitivity (m) which is reciprocal of stress exponent (n) of Zr-BMGs, becoming independent of loading strain rate when the indentation depth cross 50 nm [18]. Creep deformation mechanisms in BMGs were explained by theories like shear band formation (STZ) and free volume due non-crystalline nature of BMGs.

A very few studies have reported on creep behavior of as-cast and annealed bulk metallic glasses [20,21]. The creep of Cu-Zr and Zr BMGs is strongly affected by stress- relaxation/annealing. The annihilation of defects reduce the free volume in the Cu-Zr BMGs during annealing significantly influenced the creep properties of BMGs [20,21]. However, these studied are limited to cast BMGs in

* Corresponding author.
E-mail address: agarwala@fiu.edu (A. Agarwal).

http://dx.doi.org/10.1016/j.msea.2016.02.030
0921-5093/

Cu molds.

In the present study, creep behavior of *cold sprayed Al based BMG coatings* has been reported. It is emphasized that novelty of this study stems from the fact that creep behavior of Al based BMG has never been studied. Moreover, the microstructure obtained by cold spraying is significantly different from cast BMG structure. In cold spray technique, feedstock in the powder form is accelerated to high velocity impact on the substrate and forms coating as a layered structure. Coating structure consists of weak splat boundaries, cracks and porosity which could influence the time dependent deformation behavior. In this study, thick Al-amorphous/nano-crystalline coatings are deposited on Al-6061 using cold spray technique. Coatings are heat treated just below the crystallization temperature. Creep properties of both as-sprayed and heat treated coatings are analyzed using nanoindentation technique at room temperature as a function of peak load and hold time. The results are interpreted in-terms of coating microstructure and properties.

2. Experimental details

2.1. Powder morphology and coating deposition

Aluminum amorphous/nanocrystalline powder having composition (Al-4.4Y-4.3Ni-0.9Co-0.35Sc (at%)) is deposited on Al-6061 substrate by cold spray technique. Aluminum amorphous alloy powder is obtained by gas atomization route. The powder has spherical morphology with size range from 2.5 to 45 μm with an average size of 11 μm. Coatings were deposited up to 250 μm thickness. These coatings are heat treated at 300 °C in order to study the structural stability and its influence on the properties of the coating. More details on the powder characteristics and coating deposition has been found in reports published by present authors [22,23].

2.2. Nanoindentation creep tests

All samples were polished to mirror smooth finish for creep studies. Nanoindentation tests are performed on mirror finished coating surfaces at room temperature using Hysitron TI 900 Triboindenter and a Berkovich tip. Tests are performed at peak loads of 1000, 2000 and 4000 μN. The time required to reach the peak load is fixed at 5 s. The holding time is varied at each peak loads to study the subsequent effect. The holding times are: 0, 5, 10, 20, 30, 60, 120 and 240 s. Ten tests were conducted for each condition for the sake of reproducibility of the data. Same procedure was repeated for the heat treated coatings and the data is recorded for further analysis and interpretation. The creep indentations are profiled after each test using scanning probe microscope (SPM) in TI 900 triboindenter to understand the indent morphology in as-sprayed and heat treated coatings.

3. Results and discussion

3.1. Coating structure and properties

Cross-sectional microstructure of cold sprayed Al amorphous alloy coatings in as-sprayed and heat treated conditions studied under SEM are shown in Fig. 1. Heat treated coating exhibited dense structure with less porosity (0.5%) due to solid state diffusion during heat treatment compared to as-sprayed coating (2%). XRD analysis (Fig. 2) reveals the presence of nano-crystalline α-Al FCC phase and intermetallic phases (Al_3Y, Al_3Sc, Al_4YNi and Al_9Co_2) in the heat treated coating against broadened peaks and

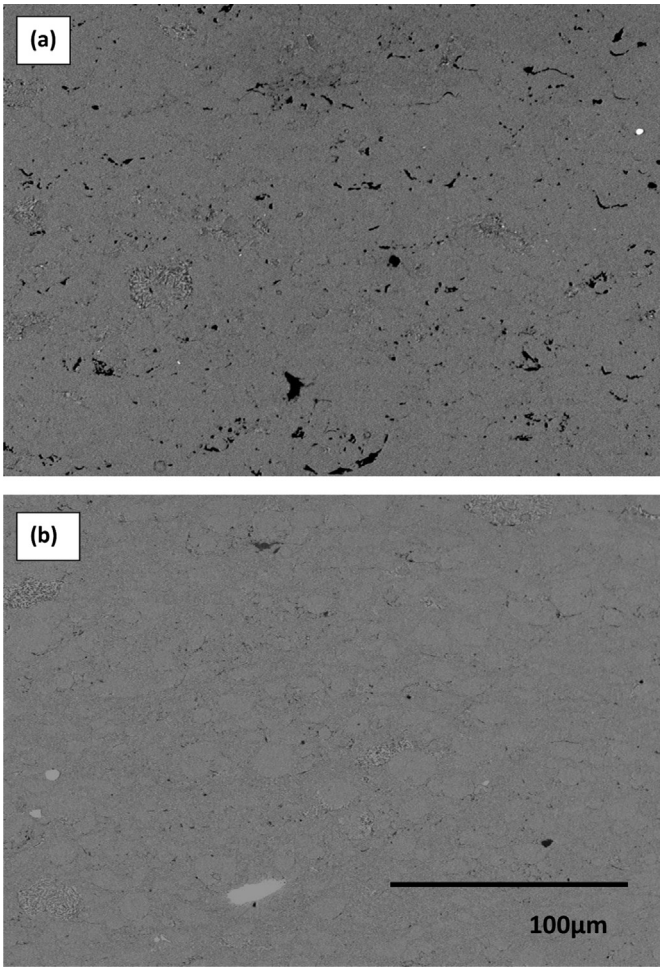

Fig. 1. Cross sectional SEM images of cold sprayed Al amorphous alloy coatings (a) as-sprayed (AS) and (b) heat treated (HT) conditions.

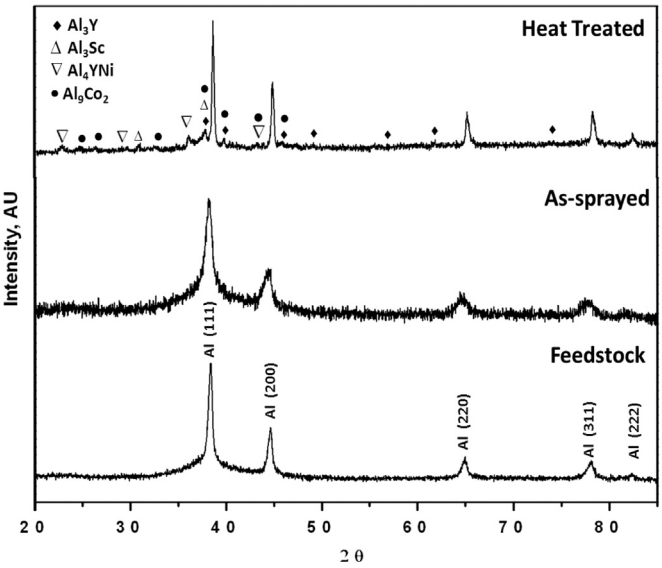

Fig. 2. X-ray diffraction patterns of initial powder feedstock, as-sprayed and heat treated (HT) Al amorphous coatings.

nano-crystalline α-Al FCC phase peaks in as-sprayed coating. Hardness and modulus of coatings are measured using nanoindentation technique. Heat treated coatings exhibited slightly higher hardness of 5.25 GPa against 5 GPa in as-sprayed coatings.

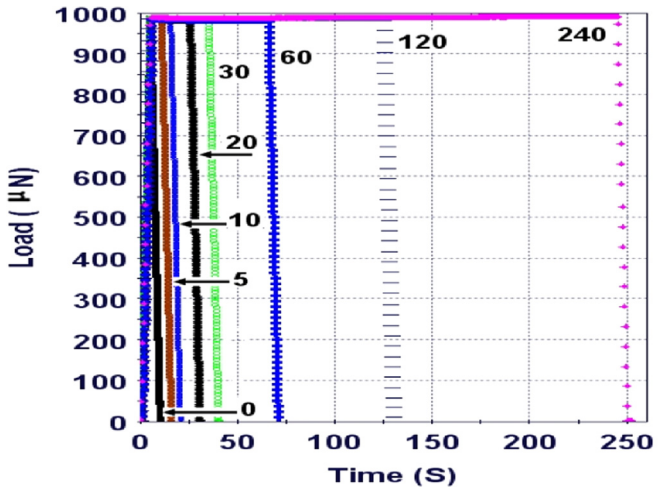

Fig. 3. Load-time cycles of nano-indentation creep tests on as-sprayed and heat treated Al amorphous alloy coatings.

Modulus of heat treated coatings (115 GPa) has improved by 33% than as-sprayed coatings (86 GPa). Partial crystallization and dense structure after heat treatment enhanced the modulus. A detailed discussion on the microstructure, phase content and mechanical properties of cold sprayed Al amorphous/nanocrystalline coatings in as-sprayed and heat treated conditions is reported in our previous publications [22,23]. This brief description is provided for the sake of better understanding for the readers.

3.2. Nanoindentation creep and coating parameters

Nanoindentation creep tests are carried out at different loads and holding times under constant load condition and typical load cycle at 1000 μN load is shown in Fig. 3. Representative load-displacement curves of as-sprayed and heat treated coatings during nanoindentation creep tests at 4000 μN peak load and 240 s holding time are shown in Fig. 4. It is very clear from the plot that the creep displacement is more pronounced in as-sprayed coating as compared to heat treated coating. It indicates that the structure relaxation after hear treatment not only influences the static properties of coatings [22,23] but also creep deformation of cold sprayed Al amorphous/nano-crystalline coatings.

Stress exponent (n) factor is most widely used to describe the time-dependent deformation in metallic materials as it provides useful information about the creep mechanisms involved. It is expressed by the well-known power law equation for steady state creep [24–26]:

$$\dot{\varepsilon}=A\sigma^{n} \tag{1}$$

where, $\dot{\varepsilon}$ is the indentation strain rate, σ is the mean stress under the indenter (hardness in the present case), the factor A is temperature dependent material constant, and n is the stress exponent can be derived as [24]:

$$n=\frac{\partial \ln(\dot{\varepsilon})}{\partial \ln(\sigma)} \tag{2}$$

In a self-similar indentation like Berkovich indenters, stress (σ), strain can be defined as [27]

$$\sigma=\frac{P}{24.5*h_c^{2}} \tag{3}$$

$$\dot{\varepsilon}=\frac{1}{h}\frac{dh}{dt}=\frac{\dot{h}}{h} \tag{4}$$

where P is the applied load, h is the instantaneous indentation depth, and the displacement rate $\dot{h}=\frac{dh}{dt}$, which is calculated by fitting the creep displacement-holding time at constant load using an empirical equation [15,24,28]:

$$h(t)=h_0+a(t-t_0)^{b}+kt \tag{5}$$

where h_o, a, t_o, b, and k are fitting constants.

The displacement vs time data was analyzed using above mentioned theory. The load-creep displacement values for as-sprayed and heat treated coatings at peak load of 1000, 2000 and 4000 μN and maximum hold time of 240 s are shown in Fig. 5. The creep displacement increased with increase in load. The creep displacement data has been fitted with empirical equation (Eq.

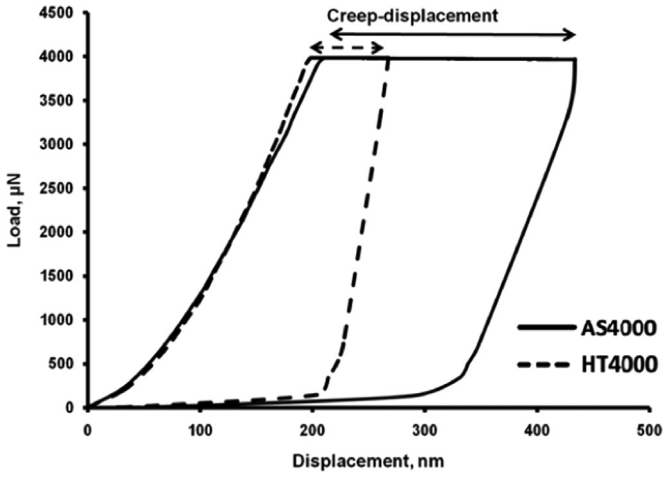

Fig. 4. Load-displacement curves at 4000 μN load and 240 s hold time on as-sprayed (AS) and heat treated (HT) cold sprayed Al amorphous alloy coatings.

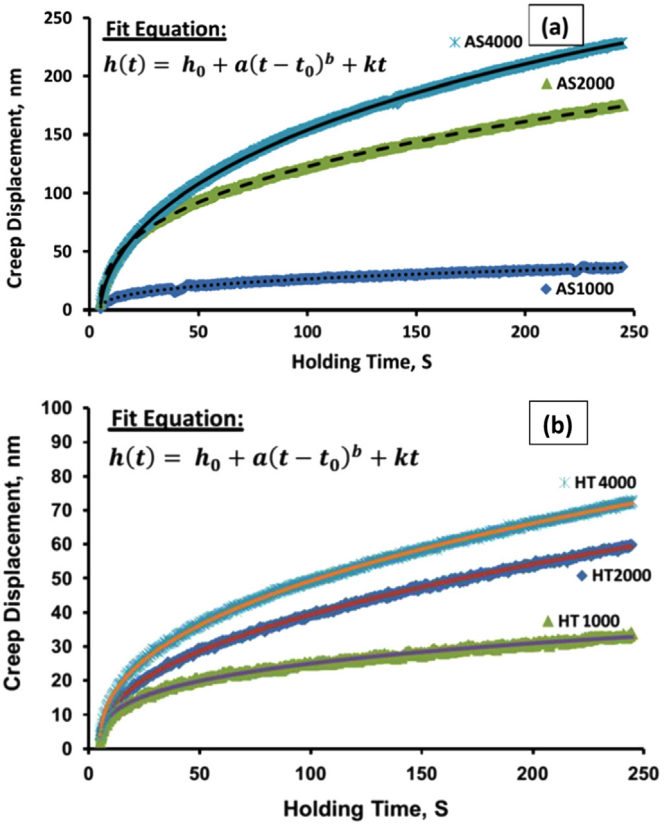

Fig. 5. Creep displacement as a function of holding time for (a) as-sprayed and (b) heat treated coatings at different loads.

Table 1
Fitting parameters of the fitted equation over experimental (creep displacement-time) data for As-sprayed and Heat treated coatings.

	As-sprayed			Heat-treated		
	AS_1000	**AS_2000**	**AS_4000**	**HT_1000**	**HT_2000**	**HT_4000**
ho, nm	87.858445	171.9439	204.7837	92.796397	133.042285	194.4249
to, s	4.9316	4.9316	4.9316	4.9316	4.9316	4.9316
a	5.02258	21.13924	15.41409	5.915076	5.580765	7.580072
b	0.378086	0.389409	0.551061	0.323538	0.405848	0.410573
k	−0.01501	−0.01668	−0.35558	−0.0082	0.021427	0.000242
R^2	0.996278	0.999374	0.999882	0.996766	0.999598	0.99971

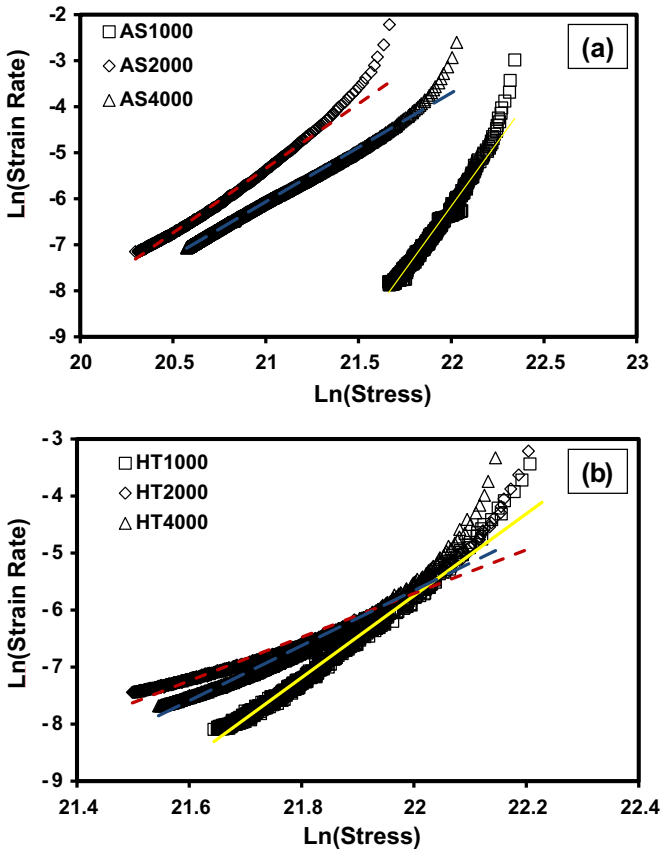

Fig. 6. Logarithmic strain rate vs. stress plots of (a) as-sprayed (AS) and (b) heat treated (HT) coatings at 240 s hold time.

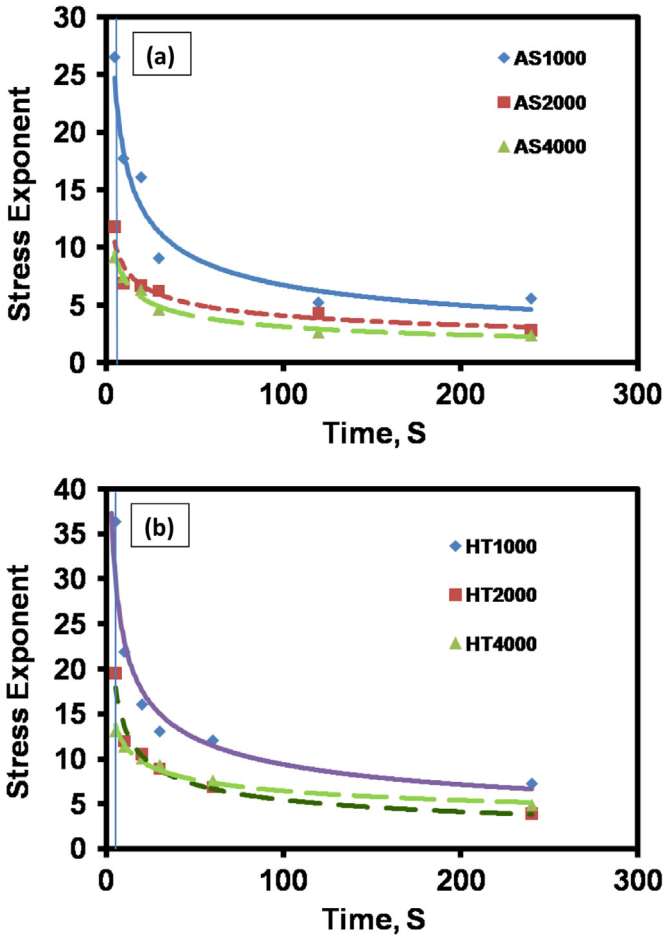

Fig. 7. Stress exponent as a function of hold time (a) AS and (b) HT coatings. A vertical line corresponding to stress exponent measurements at 5 s holding time.

(5)) for all test loads (solid lines in Fig. 5) and 240 s hold time. Similar analysis was also carried out for other peak loads and hold times. Eq. (5) fits very well ($R^2 > 0.99$) with the hold time- displacement values in the present study and fit values are shown in Table 1.

Fig. 6 shows the logarithmic strain rate ($\dot{\varepsilon}$) vs stress (σ) plots of as-sprayed and heat treated coatings. The slope of curves decreased gradually with holding time and reached linear value at the end of the holding time in each test. The stress exponent value (n) is taken from the slope of linear part of strain rate vs stress for each load and hold time and are plotted as shown in Fig. 7. The plots show higher stress exponent values as high as 26 and 36 at 1000 μN and 9 and 13 at 4000 μN for as-sprayed and heat treated coatings respectively at 5 s holding time. Stress exponent (n) becomes constant at higher holding times for all test load ranges. Similar behavior was observed by Su et al., in their experimental studies and FEM simulation [29]. Initial transient in the creep behavior is due to influence of elastic deformation and from a more complex uniaxial constitutive relation which cannot be easily described by simpler power law with unique stress exponent [29]. Hence, the stress exponent values of as-sprayed and heat treated coatings at highest holding time (240 s-in the steady state creep region) are considered for further discussion in the present study and are shown in Fig. 8 (Table 2). The stress exponent value of tests at 240 s hold time is higher at 1000 μN load (5.6(AS) and 7.2(HT)) and is less at 2000 μN (2.8(AS) and 3.8(HT)) and 4000 μN (2.3(AS) and 4.8(HT)) loads. It is clear from Fig. 8 that heat treated (HT) coatings exhibited higher stress exponent at all loads as compared to as-sprayed (AS) coatings indicating more resistance to creep deformation.

In conventional creep behavior of metallic materials, when $n \geq 4$, the dominant creep mechanisms are diffusion-controlled generation and movement of dislocations within the grains and by grain boundary sliding [30]. Lower stress exponent values like 1–2 correspond to diffusion dominated creep processes [31]. Such an

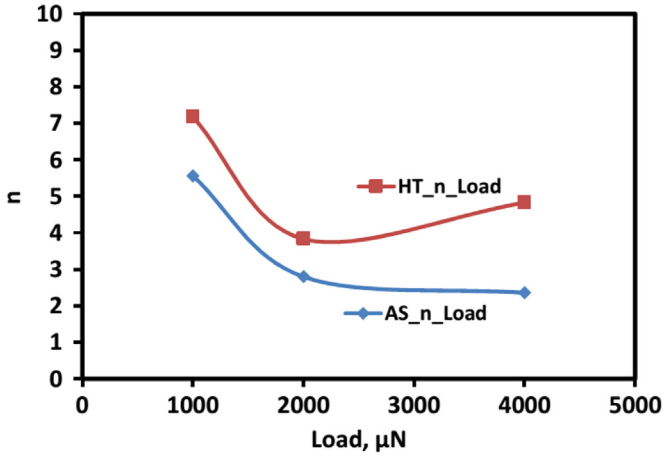

Fig. 8. Stress exponent values of coatings at 240 s hold time as a function of peak loads.

understanding is very poor in BMGs as they don't have crystalline structure and grain/grain boundary structure. The observed stress exponent values from creep tests on as-sprayed and heat treated coatings can be explained based on two aspects: (i) intrinsic properties of Al amorphous/nano-crystalline coatings in as-sprayed and heat treated conditions [20,21,23] and (ii) nature of cold sprayed microstructure [32]. Lower stress exponent values observed in as-sprayed coatings is attributed to most common deformation mechanism reported in BMGs i.e. shear band formation and propagation (shear transition zone (STZ). The higher free volume because of amorphous structure in as-sprayed coatings is also responsible for lower stress exponent values in as-sprayed coatings. In the case of heat treated coatings, the relaxed and partially crystallized structure with intermetallic phases [22,23] restricts the STZ movement. Further, annealing annihilates the defects present in the initial amorphous structure (intrinsic) of as-sprayed coating and coating becomes dense. Coating structure, like the presence of splat boundaries, porosity and particle deformation during impact may also influence the creep deformation. Annealing reduces porosity and weak inter-splat boundaries present in the as-sprayed coatings results in relaxed and less defect structure and hence the observed higher stress exponent value in heat treated coatings compared to as-sprayed coatings.

As stress exponent (n) varied as a function of holding time, stress exponent values also varied as a function of peak load (Figs. 7 and 8). Higher stress exponent values of almost double (Fig. 8 and Table 2) were noticed at 1000 μN peak load indentation creep compared to stress exponent values at 2000 and 4000 μN peak loads in both as-sprayed and heat treated coatings. This can be explained based on the peak load and loading rate used in the present. In the present study, time required to reach peak load was kept constant i.e. 5 s. It means both peak load (1000, 2000 and 4000 μN) and loading rates (100, 200 and 400 μN/s for 1000, 2000 and 4000 μN respectively) varied simultaneously in the creep tests. This provides an understanding of combine effect of both peak load and loading rate on the creep deformation (stress exponent (n)) in Al amorphous/nano-crystalline coatings. The higher stress exponent value at low load (1000 μN) may be due to very low deformation volume (indentation size effect (ISE)) under indentation compared to higher loads of 2000 μN and 4000 μN. ISE is observed in many BMGs, single crystal, nano-crystalline and coarse grain materials subjected to indentation creep tests to different depths [18]. In addition, the loading rate may also contribute to the observed decrease in stress exponent value due to increase in loading rate with increase in peak load [17,20]. However, such an understanding of lading rate on stress exponent value obtained from indentation creep studies on BMGs is very poor. For example, for same peak load of 50 mN, an increase in stress exponent value is noticed in as-cast Cu-Fe BMG for loading rates from 0.1 mN/s to 2.5 mN/s; in contrast, a decrease in stress exponent value with increase in loading rate form 1 mN/s to 50 mN/s was noticed in Fe BMG [17,20]. However, in the present study the variation in stress exponent value is very less (20–25%) in coatings when tested at 2000 and 4000 μN compared to coatings tested at 1000 μN). This support the peak load dependency on observed stress exponent (n) on indentation creep of Al amorphous/nano-crystalline coatings in the load range used in the present study is dominant as compared to loading rate. This is consistence with the constant stress exponent value (strain rate sensitivity) observed after initial shallow depths in Zr BMGs tested to different initial creep depths and loading rates [18]. The variation in 'n' value at higher peak loads i.e. 2000 and 4000 μN may also be due intrinsic coating structure like more disordered structure in one splat compared to other as present in initial powder feedstock showing more disordered structure in finer particles due to rapid cooling during atomization. *This discussion indicates that stress exponent alone is not sufficient to understand the indentation creep deformation mechanisms in cold sprayed Al amorphous/nano-crystalline coatings.*

In order to get more insight into the creep deformation mechanisms in cold sprayed Al amorphous/nano-crystalline coatings, activation volume (V*) is calculated. Activation volume also helps in the confirmation of creep mechanisms discussed above based on the stress exponent values. The macroscopic activation volume is defined as [21]:

$$V^* = k_B T \frac{\partial \ln \dot{\varepsilon}}{\partial \tau} \tag{6}$$

where, τ is the (shear) flow stress and $\dot{\varepsilon}$ is the strain rate, k_B is the Boltzmann constant, and T is the test temperature (298 K) in the present study. Based on relationship between flow stress and shear stress ($\tau = \sigma/2$) and flow stress to hardness (~2.8) and strain exponent m_H to m_σ (~0.9), Eq. (6) can be written in terms of strain exponent and hardness of coatings by following equation [21],

$$V^* = 5.1\, k_B T / m_H H \tag{7}$$

where, m_H is the strain rate sensitivity (m) (Table 2) and H is the coating hardness. The activation volume calculated from the above equation is around 98 Å^3 for as-sprayed coatings and 196 Å^3 for heat treated coatings. It means the activation volume is around 5–6 atomic volume in as-sprayed and 12–13 atomic volumes in heat treated coatings if the lattice parameter of Al amorphous alloy is assumed to be close to pure Al (4 Å) [33]. The activation volume observed in the coatings is in the order of few shear zones (simultaneous shearing a group of 10–100 atoms) in the BMGs. Similar trend is observed in earliest studies on Zr-based bulk

Table 2
Stress exponent factor and strain rate sensitivity of cold sprayed Al amorphous/nano-crystalline coatings at 240 s holding time.

	AS_1000	AS_2000	AS_4000	HT_1000	HT_2000	HT_4000
Stress exponent factor, n	5.57	2.80	2.36	7.19	3.83	4.83
Strain rate sensitivity, m	0.18	0.35	0.42	0.14	0.24	0.20

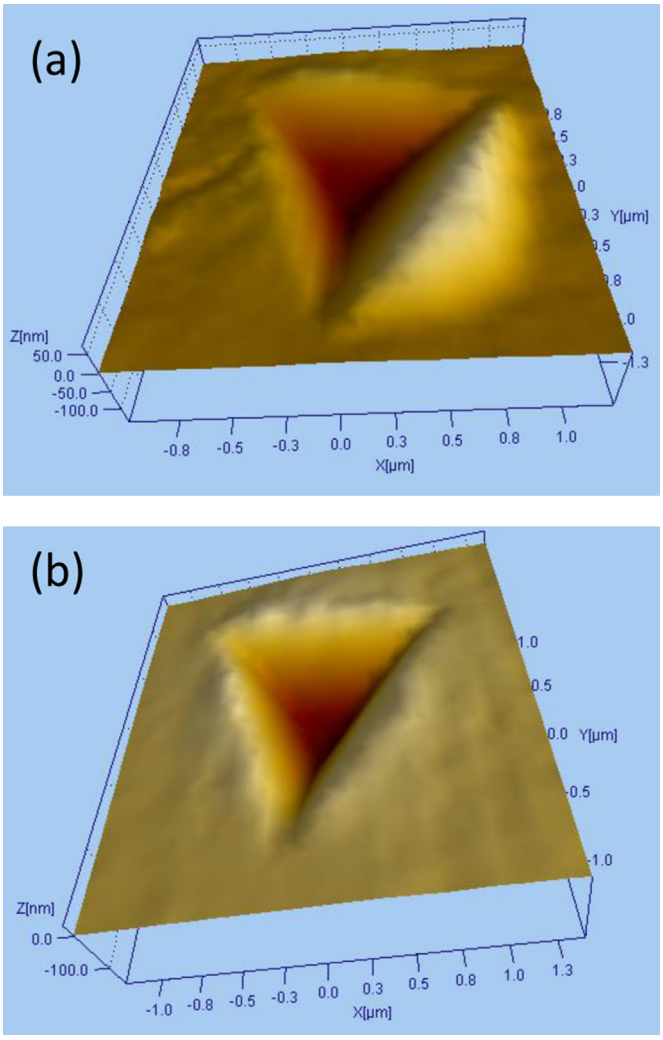

Fig. 9. Creep indentation profiles of (a) as-sprayed and (b) heat treated coatings at 4000 μN and 240 s hold time.

metallic glass in as-cast and heat treated conditions [21]. The structural relaxation during the annealing of as-sprayed coatings annihilate the defects in the coating (initial free volume) and thus results in dense packing structure at small length scales in the heat treated coatings. Hence, more atoms will take part in the deformation process under indent and result in greater resistance to creep deformation during holding period in heat treated coating. Atoms will move freely under indentation during peak load holding time in as-sprayed coating due to more random atomic packing in as-sprayed coating. Hence, activation volume helps to understand the participation of elementary units in plastic deformation of cold sprayed Al amorphous/nano-crystalline coatings confirms the creep mechanisms described based on stress exponent values.

Creep indentation profiles after tests at 4000 and 240 s hold time are shown in Fig. 9. The more material pile up is noticed in as-sprayed coatings compared to heat treated coatings. The phenomenon can be discussed based on two aspects. The depth of penetration is almost double in as-sprayed coatings compared to heat treated coatings at 4000 μN and 240 s hold time (Fig. 4) and hence more pile up is observed in the as-sprayed coatings. The second reason is attributed to smaller activation volume zone in the as-sprayed condition. The less activation zone beneath the indenter indicates the free flow of material and the more pile up in the as-sprayed coatings. In case of heat treated coatings, the dense structure not only reduced the creep rate but also the more activation zone beneath the indenter and less observed material pile up.

4. Conclusions

Nano-indentation room temperature creep behavior of cold sprayed Al amorphous/nano-crystalline coatings in as-sprayed (AS) and heat treated (HT) condition is studied. Peak load and hold time influenced the creep deformation of coatings. Higher stress exponent (n) value of 25 to 35 is found in the coatings when the hold time is around 5 s compared to 3–8 at 240 s holding time. The 'n' value decreased with increasing load at short hold periods. The 'n' values are 5.6 and 7.2 at 1000 μN load, 2.8 and 3.8 at 2000 μN and 2.3 and 4.8 at 4000 μN loads respectively in as-sprayed and heat treated coatings. Lower stress exponent values are obtained in as-sprayed coatings due to intrinsic property like more free volume, defects and extrinsic properties like weak inter splat regions, porosity, whereas the dense structure after annealing increase the resistance to creep deformation (higher stress exponent values). Activation volume i.e. atoms involved in the shear band is calculated to understand the elementary flow units responsible for creep deformation in coatings. Activation volume is double in heat treated coatings as compared to as-sprayed coatings.

Acknowledgements

Authors thankful to Dr. S. Scudino (IFW, Dresden, Germany) for providing atomized powder and Dr. J. Karthikeyan (ASB Industries, OH, USA) for assisting with cold spraying. Authors express sincere thanks to AMERI staff at FIU, Miami for maintaining the characterization facilities and providing assistance with characterization facilities.

References

[1] A.L. Geer, Partially or fully devitrified alloys for mechanical properties, Mater. Sci. Eng. A 304–306 (2001) 68–72.
[2] C.A. Schuh, T.C. Hufnagel, U. Ramamurthy, Mechanical behavior of amorphous alloys, Acta Mater. 55 (2007) 4067–4109.
[3] G. Lin, W.W. Wang, X.Q. Wu, J.H. Lei, S. Yin, Crystallization and corrosion resistance of as-spun $(Al_{86}Ni_9La_5)_{98}Zr_2$ amorphous alloy, J. Alloy. Compd. 478 (2009) 763–766.
[4] A. Inoue, Amorphous, nanoquasicrystalline and nanocrystalline alloys in Al-based systems, Prog. Mater. Sci. 43 (1998) 195–520.
[5] X.P. Li, M. Yang, B.J. Wang, G.B. Schaffer, M. Qian, Crystallization behaviour and thermal stability of two aluminium-based metallic glass powder Materials, Mater. Sci. Eng. A 530 (2011) 432–439.
[6] A. Inoue, H. Kimura, Fabrications and mechanical properties of bulk amorphous, nanocrystalline, nanoquasicrystalline alloys in aluminum-based system, J. Light Met. 1 (2001) 31–41.
[7] A. Inoue, N. Matsumoto, T. Masumoto, Al–Ni–Y–Co amorphous alloys with high mechanical strengths wide supercooled liquid region and large glass-forming capacity, Mater. Trans. JIM 31 (1990) 493–500.
[8] N. Bassim, C.S. Kiminami, M.J. Kaufman, Phases formed during crystallization of amorphous $Al_{84}Y_9Ni_5Co_2$ alloy, J. Non-Cryst. Solids 273 (2000) 271–276.
[9] D.V. Louzguine, A. Inoue, Influence of a supercooled liquid on crystallization behaviour of Al–Y–Ni–Co metallic glass, Mater. Lett. 54 (2002) 75–80.
[10] A. Inoue, S. Sobu, D.V. Louzguine, H. Kimura, K. Sasamori, Ultra high strength Al-based amorphous alloys containing Sc, J. Mater. Res. 19 (2004) 1539–1543.
[11] Y.H. Kim, A. Inoue, T. Masumoto, Ultrahigh mechanical strengths of $Al_{88}Y_2Ni_{10-x}M_x$(M=Mn, Fe or Co) amorphous alloys containing nanoscale fcc-Al particles, Mater. Trans. JIM 32 (1991) 599–608.
[12] Y.H. Kim, A. Inoue, T. Masumoto, Increase in mechanical strength of Al-Y-Ni amorphous alloys by dispersion of nanoscale fcc-Al particles, Mater. Trans. JIM 32 (1991) 331–338.
[13] W.H. Li, K. Shin, C.G. Lee, B.C. Wei, T.H. Zhang, Y.Z. He, The characterization of creep and time-dependent properties of bulk metallic glasses using nanoindentation, Mater. Sci. Eng. A 478 (2008) 371–375.
[14] Y.J. Huang, Y.L. Chiu, J. Shen, J.J.J. Chen, J.F. Sun, Indentation creep of a Ti-based

metallic glass, J. Mater. Res. 24 (2009) 993–997.
[15] Y.J. Huang, J. Shen, Y.L. Chiu, J.J.J. Chen, J.F. Sun, Indentation creep of an Fe-based bulk metallic glass, Intermetallics 17 (2009) 190–194.
[16] Byung-Gil Yoo, Kyu-Sik Kim, Jun-Hak Oh, U. Ramamurty, Jae-il Jang, Room temperature creep in amorphous alloys: influence of initial strain and free volume, Scr. Mater. 63 (2010) 1205–1208.
[17] F. Xu, Z. Long, X. Deng, P. Zhang, Loading rate sensitivity of nanoindnetation creep behaviour in a Fe-based bulk metallic glass, Trans. Nonferr. Met. Soc. China 23 (2013) 1646–1651.
[18] F. Wang, J.M. Li, P. Huang, W.L. Wang, T.J. Lu, K.W. Xu, Nanoscale creep deformation in Zr-based metallic glass, Intermetallics 38 (2013) 156–160.
[19] S. Yingdi, L. Ziquan, L. Jinsong, C. Mengqi, Q. Jingya, Indentation creep behaviors of $Mg_{61}Cu_{28}Gd_{11}$ and $(Mg_{61}Cu_{28}Gd_{11})_{99.5}Sb_{0.5}$ bulk metallic glasses at room temperature, J. Rare Earths 29 (2011) 253–258.
[20] Byung-Gil Yoo, Jun-Hak Oh, Yong-Jae Kim, Kyoung-Won Park, Jae-Chul Lee, Jae-il Jang, Nanoindentation analysis of time-dependent deformation in as-cast and annealed Cu-Zr bulk metallic glass, Intermetallics 18 (2010) 1898–1901.
[21] J.B. Puthoff, D.S. Stone, H. Cao, P.M. Voyles, Change in activation volume for plastic deformation of Zr-based bulk metallic glass following annealing, Mater. Res. Soc. Symp. Proc. 1048 (2008) 1048-Z03-08.
[22] D. Lahiri, P.K. Gill, S. Scudino, C. Zhang, V. Singh, J. Karthikeyan, N. Munroe, S. Seal, Arvind Agarwal, Cold sprayed aluminum based glassy coating: synthesis, wear and corrosion properties, Surf. Coat. Technol. 232 (2013) 33–40, http://dx.doi.org/10.1016/j.surfcoat.2013.04.049.
[23] P. Suresh Babu, Debrupa Lahiri, G. Sundararajan, Arvind Agarwal, Scratch induced deformation behavior of cold sprayed aluminum amorphous/nanocrystalline coatings at multiple load scales, J. Therm. Spray Technol. 23 (2016) 502–513.
[24] K. Johnson, Contact Mechanics, Cambridge University Press, Cambridge, 1985.
[25] A.F. Bower, N.A. Fleck, A. Needleman, N. Ogboma, Indentation of a power law creeping solid, Proc. R. Soc. Lond. Ser. A – Math. Phys. Eng. Sci. 441 (1993) 97–124.
[26] J. Wu, Y. Pan, J. Pi, On indentation creep of two Cu-based bulk metallic glasses via nanoindnetation, Phys. B: Condens. Matter 421 (2013) 57–62.
[27] B.N. Lucas, W.C. Oliver, Indentation power-law creep of high-purity indium, Metall. Mater. Trans. A 30 (1999) 601–610.
[28] H. Li, A.H.W. Ngan, Size effects of nanoindentation creep, J. Mater. Res. 19 (2004) 513–522.
[29] Caijun Su, Measurement of Power-law creep parameters by instrumented indentation methods (Ph.D dissertation), University of Tennessee, 2012.
[30] V. Sklenicka, J. Dvorak, M. SSvoboda, Creep in ultrafine grained aluminium, Mater. Sci. Eng. A 387–389 (2004) 696–701.
[31] R. Mahmudi, A.R. Geranmayeh, H. Khanbareh, N. Jahangiri, Indentation creep of lead-free Sn–9Zn and Sn–8Zn–3Bi solder alloys, Mater. Des. 30 (2009) 574–580.
[32] Thomas W. Reza Soltani, Coyle, Javad Mostaghimiy, Creep behavior of plasma-sprayed zirconia thermal barrier coatings, J. Am. Ceram. Soc. 90 (9) (2007) 2873–2878.
[33] D. Nagahama, T. Ohkubo, T. Mukai, K. Hono, Characterization of nanocrystal dispersed $Cu_{60}Zr_{30}Ti_{10}$ metallic glass, Mater. Trans. 46 (2005) 1264–1270.